

Evaluation of Potency and Specificity of Cryptophycin-Loaded Antibody-Drug Conjugates

Peter Bitsch,^[a] Cedric Dessin,^[b] Sebastian Bitsch,^[a] Jona Voss,^[b] Janine Becker,^[a] Panna Sharma,^[c] Neha Biyani,^[c] Harry Kochat,^[d] Norbert Sewald,^{*,[b]} and Harald Kolmar^{*,[a, e]}

An enhanced variant of the antimetabolic toxin cryptophycin was conjugated to the anti-Her2 monoclonal antibody (mAb) Trastuzumab upon Michael addition. Either antibodies with freed hinge-region cysteines or THIOMAB formats with engineered cysteines in the mAbs light chain were added to a maleimide derivative of cryptophycin. These Antibody-Drug Conjugates (ADCs) showed retained binding to Her2 positive tumor cells and highly efficient cell killing in double-digit pM range on high Her2-expressing SK-BR-3 cells. Two ADCs (DAR 6,

DAR 3) showed superior cell killing of the cell lines JIMT-1 and RT112 with medium receptor expression level in comparison with a DAR 6 MMAE ADC serving as reference. The observed cell cytotoxicity is target-dependent since no impact on cell viability was observed for low Her2-expressing MDA-MB468 cells. Particularly the DAR 3 ADC in THIOMAB format exhibiting desirable biophysical properties and high potency emerged as a promising candidate for further *in vivo* investigations.

Introduction

Inspired by Paul Ehrlich's idea of a 'magic bullet',^[1] antibody-drug-conjugates (ADCs) have evolved to become promising modalities in cancer therapy to support or substitute chemotherapy, radiotherapy or immunotherapy with already 15 ADCs^[2] approved by the Food and Drug Administration (FDA) and more than 160 candidates in clinical trials.^[3] ADCs comprise a monoclonal antibody (mAb) for targeting antigens highly presented by cells in malignant tissue, a linker molecule and a cytotoxic drug. Multiple variants of linkers are available, whereas most of the approved and clinically tested ADCs comprise cleavable linkers.^[3] These are designed in a way that they conditionally release the cytotoxic drug in the tumor micro-environment, e.g. due to lowered pH value or reducing conditions. Alternatively they allow for a proteolytic release

after uptake into tumor cells by enzymes residing in the endosome such as cathepsin B, resulting in a traceless release of the cytotoxin by using a valine-citrulline-(*p*-aminobenzyl alcohol)-linker (Val-Cit-PAB).^[4,5] Additionally, methods have been developed to release toxins by external stimuli such as light activation or 'click' chemistry.^[4,6] Linker attachment can be achieved either by chemical ligation to native or implemented conjugation handles, or by enzymatic conjugation to engineered recognition sites at the mAb.^[7] Among chemical ligation methods, addressing native lysines or hinge-region cysteines are the most prominent approaches that are already routinely utilized for generation of clinically applied ADCs. Conjugation involving cysteines typically yields more homogeneously loaded mAbs.^[3]

Broadening the therapeutic window is key to ADC design.^[8] To this end, the constructs should exhibit a significant difference between minimum effective dose (MED) and maximum tolerated dose (MTD).^[9] Merely increasing drug loading does not necessarily yield more effective ADCs due to increased hydrophobicity of the constructs, potentially leading to aggregation and degradation in plasma.^[10] Yet, utilization of more potent drugs was shown to yield more potent ADCs by lowering the MED.^[11,12] However, severe side effects were observed in clinical studies due to an associated lowered MTD.^[12] Strategies to increase MTD while maintaining or even further decreasing MED include utilization of different linkers as well as careful selection and design of antibody conjugation sites and adjustment of the drug-to-antibody ratio (DAR).^[8,13]

A class of already successfully applied toxins are antimetabolic drugs like monomethyl auristatin E (MMAE, **1**) (Figure 1 a) binding to tubulin and destabilizing microtubules.^[14] Among them, the antimetabolic depsipeptide cryptophycin (Cp) had been investigated in clinical trials for application in tumor therapy but was withdrawn due to severe side effects.^[15] Since then, efforts have been made to overcome these side effects by implementation of cryptophycins into ADC formats. Verma *et al.*


[a] P. Bitsch, S. Bitsch, J. Becker, H. Kolmar
Clemens-Schöpf Institute for Organic Chemistry and Biochemistry, Technical University of Darmstadt, Peter-Grünberg-Str. 4, 64287 Darmstadt, Germany
E-mail: Harald.Kolmar@TU-Darmstadt.de


[b] C. Dessin, J. Voss, N. Sewald
Organic and Bioorganic Chemistry, Faculty of Chemistry, University of Bielefeld, Universitätsstraße 25, 33615 Bielefeld, Deutschland
E-mail: Norbert.Sewald@uni-bielefeld.de

[c] P. Sharma, N. Biyani
Lantern Pharma Inc., 1920 McKinney Ave, 7th Floor, Dallas 75201, TX, USA

[d] H. Kochat
The University of Tennessee, Health Science Center, 208 S. Dudley Street, Memphis 38163, TN, USA

[e] H. Kolmar
Centre of Synthetic Biology, Technical University of Darmstadt, Peter-Grünberg-Str. 4, 64287 Darmstadt, Germany

 Supporting information for this article is available on the WWW under <https://doi.org/10.1002/cbic.202400738>

 © 2024 The Author(s). ChemBioChem published by Wiley-VCH GmbH. This is an open access article under the terms of the Creative Commons Attribution License, which permits use, distribution and reproduction in any medium, provided the original work is properly cited.

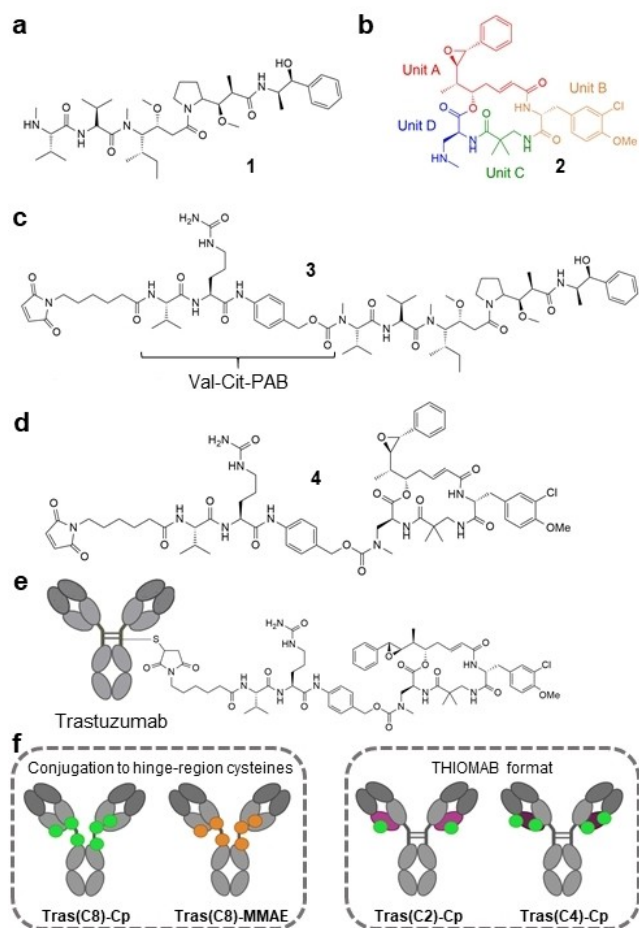


Figure 1. a: Monomethyl auristatin E 1. b: cryptophycin-uD[Dap(Me)] 2. c: Mc-Val-Cit-PAB-MMAE 3. d: Mc-Val-Cit-PAB-cryptophycin-uD[Dap(Me)] 4. e: schematic depiction of attachment of Mc-Val-Cit-PAB-cryptophycin-uD[Dap(Me)] 4 to a cysteine of trastuzumab. f: overview of generated constructs, left: **Tras(C8)-Cp** and **Tras(C8)-MMAE**, obtained via conjugation to hinge region cysteines; right: **Tras(C2)-Cp** and **Tras(C4)-Cp**, obtained via conjugation to engineered cysteines in the light chain of THIOMAB variants of trastuzumab. Created with BioRender.com.

generated cryptophycin-loaded ADCs utilizing the THIOMAB technology and obtained low picomolar potency on high Her2-expressing cell lines.^[16] Recently, Lai *et al.* synthesized a prodrug derivative of cryptophycin-52, namely cryptophycin-55, which enabled the generation of anti-Her2 ADCs based on trastuzumab with medium DARs of about 3.5.^[17] Achieving sub-nanomolar potency on high Her2-expressing cell lines SKOV3 and NCI-N78 they reported on efficient tumor growth inhibition *in vivo*. The approaches by Verma *et al.* and Lai *et al.* also demonstrate the most prominent attachment points of cryptophycins to drug conjugates being unit A with modifications of the phenyl ring or the epoxide moiety into a halohydrin. In many cases, however, modifying unit A clearly impairs cytotoxicity.^[18]

Recent findings by Wingfield *et al.*^[19] and Prota *et al.*^[20] confirmed that unit D could serve as a viable attachment point for conjugation without compromising cytotoxicity. Crystallographic studies of a cryptophycin-tubulin complex conducted

by Prota and colleagues revealed that unit D extends outward from the binding pocket, making it amenable to modifications (Figure 1b).^[20] Intrigued by these findings Dessin *et al.* designed an array of cryptophycins modified in unit D. Intense structure-activity relationship studies revealed a single-digit picomolar EC₅₀ value against KB-3-1 cells for one of the most potent congeners cryptophycin-uD[Dap(Me)] 2 (Figure 1b) which contains a secondary amino group for conjugation (Figure 1).^[21] The amino function allows for conjugation analogous to MMAE 1.

Results and Discussion

We hypothesized that the highly potent cryptophycin-derived toxin might enable effective cell killing of moderately receptor expressing cell lines that do not respond to treatment with less potent toxin-bearing ADCs usually applied. We embarked on the generation of Cp-loaded ADCs utilizing Michael addition by native cysteines of anti-Her2 mAb Trastuzumab as well as by engineered cysteine residues of two THIOMAB variants of Trastuzumab (LC Q124C and LC Q124C Q166C) (Figure 1).^[22,23] For conjugation of the drugs, 1 and 2 were modified with a maleimidocaproyl-Val-Cit-PAB (Mc-Val-Cit-PAB) linker to yield Mc-Val-Cit-PAB-MMAE 3 (Figure 1c) and Mc-Val-Cit-PAB-cryptophycin-uD[Dap(Me)] 4 (Figure 1d) to enable endosomal drug-release upon cathepsin B cleavage. Thus, 3 was utilized to generate an MMAE-loaded ADC upon conjugation to hinge-region cysteines, serving as reference molecule.

Generation of Conjugates

The attachment of the linker-toxins to Trastuzumab was performed following two different approaches. 3 and 4 were introduced to the hinge region cysteines via Michael addition to achieve a high DAR of up to 8, yielding conjugates **Tras(C8)-MMAE** and **Tras(C8)-Cp**, respectively (Figure 1f). Additionally, two THIOMAB variants of trastuzumab were produced, comprising one or two engineered cysteines in the mAb's light chain (LC) with Q124C^[23] or Q124C/Q166C^[22] exchange, respectively. These mutations allowed attachment of a distinct number of payloads at defined conjugation sites to create more homogeneous products with a maximum DAR of 2 (**Tras(C2)-Cp**) and 4 (**Tras(C4)-Cp**), respectively.

Hydrophobic interaction chromatographic (HIC) analysis confirmed the generation of different conjugates, each being more hydrophobic than their parental antibodies, exhibiting peaks at higher retention times (Figure S 1). Through analyses by size exclusion chromatography (SEC), no formation of aggregates was observed for **Tras(C2)-Cp** and **Tras(C4)-Cp**, but to some extent for **Tras(C8)-MMAE** and to high extent for **Tras(C8)-Cp** (Figure S 2). This was attributed to the fact that nearly all hinge-region cysteines were addressed by conjugation, therefore opening hydrophobic patches of the antibody in conjunction with a high copy number of the hydrophobic drug leading to aggregation.^[10,24] However, no precipitation of the purified constructs was observed and analysis three months

after generation revealed no degradation of the constructs (data not shown).

Matrix-assisted laser desorption/ionization (MALDI) mass spectrometric (MS) analysis was performed for DAR determination of all conjugates (Table S1, Figure S3). For **Tras(C2)-Cp** and **Tras(C4)-Cp** mass spectra perfectly matched the observed different ADC species from HIC analysis to be variants with DAR 0, 1 and 2. Mean DAR of the two THIOMABs was estimated to be 1.5 for **Tras(C2)-Cp** and 3 for **Tras(C4)-Cp**, respectively. For both **Tras(C8)** conjugates, mass spectra of LC and heavy chain (HC) alone as well as of the LC-HC monomer revealed the formation of all possible species from DAR 1 up to DAR 8. High DAR species were most abundant, thus the mean DAR of these conjugates was estimated to be 6.

Cellular Binding and Her2 Expression of Tested Cell Lines

Cellular binding assays were performed to assess whether the drug conjugation to the antibody hampered Trastuzumab binding to Her2 (Figure 2a). All ADCs revealed EC_{50} values on SK-BR-3 cells (Table 1) less than 10-fold higher than the unmodified Trastuzumab. Thus, both conjugation approaches did not drastically impair Her2-specific cell binding.

As no significant impact of toxin conjugation on binding behavior was observed, high Her2 expressing SK-BR-3, medium expressing JIMT-1 and RT112 and low expressing MDA-MB468 cells were chosen to conduct cellular proliferation assays. Cellular binding assays were performed to confirm the correlation between mRNA level of Her2 transcript obtained from literature^[25] and Her2 level on the cell surface. Cells were

incubated with a saturating concentration of 50 nM Trastuzumab and subsequently stained with anti-human Fc goat phycoerythrin (PE) mAb^[26]. With the stained cells, flow cytometry analyses were performed, and mean fluorescence intensities (FI) were determined (Figure 3). The highest mean FI was observed for SK-BR-3 cells as expected, being at least 4 times higher than mean FIs of JIMT-1 and RT112, MKN-45 and A549, possibly exceeding detection limits. For stained MDA-MB468 cells, nearly no fluorescent cell staining was observed. In conclusion, Her2 cell display levels matched the expectations derived from literature mRNA levels,^[25] confirming SK-BR-3 as high, JIMT-1 and RT112 as medium and MDA-MB468 as low Her2 expressing cell lines.

Cellular Proliferation Assays

Proliferation assays revealed EC_{50} values in double-digit picomolar range for all constructs on high HER2 expressing cell line SK-BR-3 (Figure 3a, Table 2) which was found to be comparable or significantly lower than for Cp-bearing ADCs found in literature.^[16,17] Along that, **Tras(C8)-Cp** and **Tras(C4)-Cp** showed similar potency, while potencies of **Tras(C2)-Cp** and **Tras(C8)-MMAE** were slightly lower. Additionally, the EC_{50} value of **Tras(C8)-MMAE** was slightly lower than the potency of a DAR 4 trastuzumab-MMAE conjugate on SK-BR-3 where the toxin was attached to a branched linker introduced upon enzyme-mediated conjugation to Q295 of a deglycosylated trastuzumab.^[27] Toxins 1 and 2 showed EC_{50} values in the expected range of high double-digit to low triple-digit picomolar values (Figure S4, Table S2), 2 being more potent than 1.^[18,28] These findings were confirmed in biological replicates.

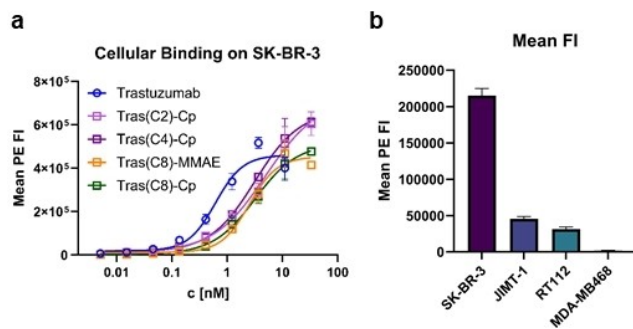


Figure 2. a Cellular binding of generated ADCs on SK-BR-3 cells. Assays were performed in triplicates. b: Mean fluorescence intensities of cells treated with 50 nM Trastuzumab and subsequently stained with α -human Fc goat PE mAb.

Construct	EC_{50} [nM]
Trastuzumab	0.6
Tras(C2)-Cp	5.0
Tras(C4)-Cp	3.2
Tras(C8)-Cp	3.2
Tras(C8)-MMAE	2.5

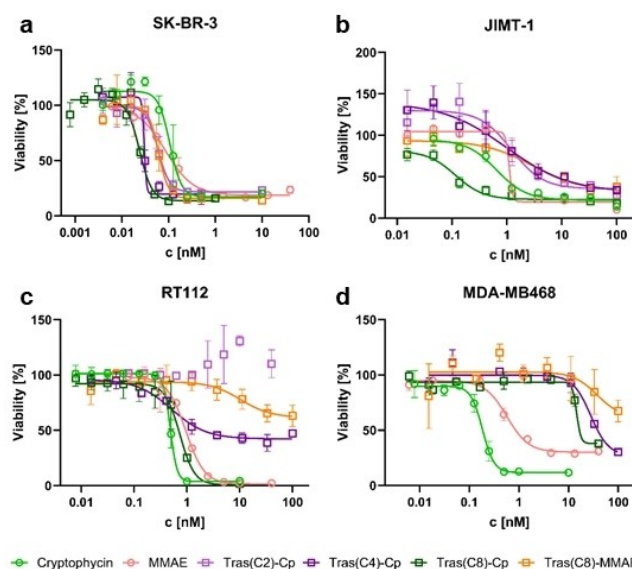


Figure 3. Results of cellular proliferation assays. All constructs were tested in technical triplicates. a: Cellular proliferation assay on SK-BR-3 cells. b: Cellular proliferation assay on JIMT-1 cells. c: Cellular proliferation assay on RT112 cells. d: Cellular proliferation assay on MDA-MB468 cells.

Table 2. EC₅₀ values and % maximum killing of constructs on all tested cell lines with corresponding 95 % confidence intervals (n.d.: not detectable).

Cell line	Construct	EC ₅₀ [pM]	Max. killing [%]
SK-BR-3	1	86 ± 30	81 ± 5
	2	107 ± 22	83 ± 8
	Tras(C2)-Cp	59 ± 10	78 ± 7
	Tras(C4)-Cp	30	80 ± 5
	Tras(C8)-Cp	24 ± 4	86 ± 8
	Tras(C8)-MMAE	61 ± 9	84 ± 7
JIMT-1	1	1100	80 ± 3
	2	646 ± 219	78 ± 5
	Tras(C2)-Cp	1208 ± 452	64 ± 14
	Tras(C4)-Cp	982 ± 899	69 ± 16
	Tras(C8)-Cp	115 ± 48	77 ± 4
	Tras(C8)-MMAE	2940 ± 1674	67 ± 10
RT112	1	948 ± 135	98 ± 5
	2	483 ± 28	96 ± 5
	Tras(C2)-Cp	n.d.	n.d.
	Tras(C4)-Cp	515 ± 195	58 ± 4
	Tras(C8)-Cp	732 ± 215	99 ± 22
	Tras(C8)-MMAE	10370 ± 6865	38 ± 10
MDA-MB468	1	572 ± 86	70 ± 3
	2	184 ± 15	88 ± 5
	Tras(C4)-Cp	n.d.	n.d.
	Tras(C8)-Cp	n.d.	n.d.
	Tras(C8)-MMAE	n.d.	n.d.

Cellular proliferation assays conducted on the cell line JIMT-1 with medium Her2 expression revealed EC₅₀ = 115 pM for **Tras(C8)-Cp**, which was approximately ten times lower than the EC₅₀ values of all other conjugates (Figure 3 b, Table 2). Additionally, both THIOMAB variants equipped with cryptophycin 2 showed higher potency than **Tras(C8)-MMAE**, indicating superior potency of cryptophycin-uD[Dap(Me)] 2 in comparison to MMAE 1. This difference in potency was also observed by comparison of cell killing ability of unconjugated toxins as 2 showed lower EC₅₀ values than 1.

Similar to the results of viability assays conducted on JIMT-1 cells, **Tras(C8)-Cp** also showed superior potency in comparison with all other ADCs on RT112 cells (Figure 3c, Table 2). Additionally, **Tras(C4)-Cp** showed an apparently equal EC₅₀ value to **Tras(C8)-Cp** but exhibited only cytostatic effects. Furthermore, no toxicity was observed for **Tras(C2)-Cp** and only low cytostatic effects for **Tras(C8)-MMAE** with double-digit nM EC₅₀ values. Comparison of bare toxins again revealed slightly higher potency for 2 revealed than for 1. These observations show the potential of the novel cryptophycin-uD[Dap(Me)] 2 as toxin for ADC application. Tumor cells with medium antigen expression levels could still be addressed and successfully treated, especially utilizing the **Tras(C8)-format**. The observations made for 1, 2 and **Tras(C8)-Cp** tested on RT112 were confirmed by biological replicates as well (Figure S5, Table S3).

On low Her2 expressing cell line MDA-MB468, no ADC showed significant cytotoxicity, except for **Tras(C8)-Cp** in the highest tested concentrations (Figure 3d, Table 2). Having cytotoxic effects on a low antigen expressing cell line might impede application of a construct in clinic as the risk of induced side effects on healthy tissue increases. On the other hand, for FDA approved trastuzumab emtansin and trastuzumab deruxtecan toxicity on MDA-MB468 cells was also described to be in the double-digit nanomolar range but both therapeutics still maintained a reliable therapeutic index.^[29] Again, 1 exhibited lower potency and max killing compared to 2.

Conclusions

In general, cryptophycin-uD[Dap(Me)] 2 with a secondary amino group in unit D showed highly efficient cell killing on every tested cell line expressing medium to high levels of Her2, always in sub-nanomolar range and with high % maximum killing of over 80% in most cases, thus outperforming the MMAE reference. All generated ADCs showed double-digit picomolar potency in high Her2 expressing SK-BR-3 cells, but differences between the constructs could be observed by treating moderate Her2 expressing cell lines. Thus, **Tras(C8)-Cp** appeared to be more potent than the lower DAR variants when tested on RT112 and JIMT-1. Most importantly, it also showed significantly higher potency than its MMAE counterpart **Tras(C8)-MMAE**. The reason for the higher potency of cryptophycin-uD[Dap(Me)] 2 versus MMAE 1 remains to be elucidated. It may be caused among other possibilities by higher affinity to tubulin^[30,31] or less efficient export. Thus, MMAE 1 has been reported to be a substrate for the efflux transporter P-gp-MDR1 and cell lines that highly express P-gp-MDR1 showed higher EC₅₀ values towards the cytotoxic effects of MMAE 1.^[32] In general, cryptophycins are assumed to be poor substrates of drug efflux pumps.^[30,33] Indeed, cryptophycin-uD[Dap(Me)] 2 showed extraordinarily low EC₅₀ values against both the human cervix carcinoma cell line KB-3-1 (8.71 pM) and its multi-drug resistant subclone KB-V1 (21.5 nM) with a resistance factor of about 2500,^[21] hinting to inefficient cellular export by the drug efflux system. Likewise, the reason for differences in potency of both cryptophycin-uD[Dap(Me)] 2 and MMAE 1 towards various cell lines requires further investigation. However, this remains to be proven for the specific cryptophycin and it will require further experimental exploration whether similar or different pathways account for the export of cryptophycin-uD[Dap(Me)] 2 compared to MMAE 1. Notably, while previous animal studies with a cryptophycin-loaded ADC look promising,^[17] detailed further studies are required that should include tumor models with medium Her2 expression to find the right balance between on-tumor potency and off-target toxicity.

Funding

Lantern Pharma Inc. had no role in the study design, data collection and analysis, interpretation of data, decision to

publish, or preparation of the manuscript. All authors had a role in study design, data collection and analysis, interpretation of data, decision to publish, or preparation of the manuscript.

The authors acknowledge support by the mass spectrometry core facility team of the Chemistry Department (TU Darmstadt) for measurements of the MALDI mass spectra and the German Research Foundation (DFG) through grant no INST 163/445-1 FUGG (MALDI MS). The authors also thank Lantern Pharma Inc for their input of expertise and support on many levels.

Conflict of Interests

PS, NB, and HK (Kochat) have been salaried employees of or consultants to Lantern Pharma Inc., TX, USA.

Data Availability Statement

The data that support the findings of this study are available in the supplementary material of this article.

Keywords: ADC · Cryptophycin · MMAE · Trastuzumab · THIOMAB

- [1] K. Strebhardt, A. Ullrich, *Nat. Rev. Cancer* **2008**, *8*, 473–480.
- [2] Z. Wang, H. Li, L. Gou, W. Li, Y. Wang, *Acta Pharm. Sin. B* **2023**, *13*, 4025–4059.
- [3] H. Maecker, V. Jonnalagadda, S. Bhakta, V. Jammalamadaka, J. R. Junutula, *mAbs* **2023**, *15*, 2229101.
- [4] A. Dal Corso, L. Pignataro, L. Belvisi, C. Gennari, *Chem. Eur. J.* **2019**, *25*, 14740–14757.
- [5] a) R. V. J. Chari, M. L. Miller, W. C. Widdison, *Angew. Chem. Int. Ed.* **2014**, *53*, 3796–3827; b) G. M. Dubowchik, R. A. Firestone, L. Padilla, D. Willner, S. J. Hofstead, K. Mosure, J. O. Knipe, S. J. Lasch, P. A. Trail, *Bioconjug. Chem.* **2002**, *13*, 855–869.
- [6] a) T. L. Rapp, C. A. DeForest, *Adv. Drug Deliv. Rev.* **2021**, *171*, 94–107; b) R. Rossin, R. M. Versteegen, J. Wu, A. Khasanov, H. J. Wessels, E. J. Steenbergen, W. ten Hoeve, H. M. Janssen, A. H. A. M. van Onzen, P. J. Hudson, M. S. Robillard, *Nat. Commun.* **2018**, *9*, 1484.
- [7] a) H. Schneider, L. Deweid, O. Avrutina, H. Kolmar, *Anal. Biochem.* **2020**, *595*, 113615; b) K. Tsuchikama, Z. An, *Protein Cell* **2018**, *9*, 33–46.
- [8] T. D. Nguyen, B. M. Bordeau, J. P. Balthasar, *Cancersp.* **2023**, *15*, 713.
- [9] H.-P. Gerber, S. Gangwar, A. Betts, *mAbs* **2023**, *15*, 2230618.
- [10] J. W. Buecheler, M. Winzer, J. Tonillo, C. Weber, H. Gieseler, *Mol. Pharm.* **2018**, *15*, 2656–2664.
- [11] A. Beck, L. Goetsch, C. Dumontet, N. Corvaia, *Nat. Rev. Drug Discov.* **2017**, *16*, 315–337.
- [12] B. E. de Goeij, J. M. Lambert, *Curr. Opin. Immunol.* **2016**, *40*, 14–23.
- [13] J. R. Junutula, H. Raab, S. Clark, S. Bhakta, D. D. Leipold, S. Weir, Y. Chen, M. Simpson, S. P. Tsai, M. S. Dennis, Y. Lu, Y. G. Meng, C. Ng, J. Yang, C. C. Lee, E. Duenas, J. Gorrell, V. Katta, A. Kim, K. McDorman, K. Flagella, R. Venook, S. Ross, S. D. Spencer, W. Lee Wong, H. B. Lowman, R. Vandlen, M. X. Sliwkowski, R. H. Scheller, P. Polakis, W. Mallet, *Nat. Biotechnol.* **2008**, *26*, 925–932.
- [14] J. A. Francisco, C. G. Cerveny, D. L. Meyer, B. J. Mixan, K. Klussman, D. F. Chace, S. X. Rejniak, K. A. Gordon, R. DeBlanc, B. E. Toki, C.-L. Law, S. O. Doronina, C. B. Siegall, P. D. Senter, A. F. Wahl, *Blood* **2003**, *102*, 1458–1465.
- [15] a) J. J. Field, A. Kanakkanthara, J. H. Miller, *Bioorg. Med. Chem.* **2014**, *22*, 5050–5059; b) C. Shih, B. A. Teicher, *Curr. Pharm. Des.* **2001**, *7*, 1259–1276.
- [16] V. A. Verma, T. H. Pillow, L. DePalatis, G. Li, G. L. Phillips, A. G. Polson, H. E. Raab, S. Spencer, B. Zheng, *Bioorg. Med. Chem. Lett.* **2015**, *25*, 864–868.
- [17] Q. Lai, M. Wu, R. Wang, W. Lai, Y. Tao, Y. Lu, Y. Wang, L. Yu, R. Zhang, Y. Peng, X. Jiang, Y. Fu, X. Wang, Z. Zhang, C. Guo, W. Liao, Y. Zhang, T. Kang, H. Chen, Y. Yao, L. Gou, J. Yang, *Eur. J. Med. Chem.* **2020**, *199*, 112364.
- [18] C. Weiss, E. Figueras, A. N. Borbely, N. Sewald, *J. Pept. Sci.* **2017**, *23*, 514–531.
- [19] E. Eren, N. R. Watts, D. L. Sackett, P. T. Wingfield, *J. Biol. Chem.* **2021**, *297*, 101138.
- [20] A.-C. Abel, T. Mühlethaler, C. Dessin, T. Schachtsiek, B. Sammet, T. Sharpe, M. O. Steinmetz, N. Sewald, A. E. Prota, *J. Biol. Chem.* **2024**, *300*, 107363.
- [21] C. Dessin, T. Schachtsiek, J. Voss, A.-C. Abel, B. Neumann, H.-G. Stammer, A. E. Prota, N. Sewald, *Angew. Chem. Int. Ed.* **2024**, e202416210.
- [22] M. Li, C. Song, J. Li, J. Min, L. Cao, L. Wang, N. Ma, *ChemBiochem* **2023**, *24*, e202200780.
- [23] D. Shinmi, E. Taguchi, J. Iwano, T. Yamaguchi, K. Masuda, J. Enokizono, Y. Shiraishi, *Bioconjug. Chem.* **2016**, *27*, 1324–1331.
- [24] R. G. E. Coumans, G. J. A. Ariaans, H. J. Spijker, P. Renart Verkerk, P. H. Beusker, B. P. A. Kokke, J. Schouten, M. Blomenröhr, M. M. C. van der Lee, P. G. Groothuis, R. Ubink, W. H. A. Dokter, C. M. Timmers, *Bioconjug. Chem.* **2020**, *31*, 21362146.
- [25] “Cell line - ERBB2 - The Human Protein Atlas”, to be found under <https://www.proteinatlas.org/ENSG00000141736-ERBB2/cell+line>, **2024**.
- [26] S. W. Jarantow, B. S. Bushey, J. R. Pardinias, K. Boakye, E. R. Lacy, R. Sanders, M. A. Sepulveda, S. L. Moores, M. L. Chiu, *J. Biol. Chem.* **2015**, *290*, 24689–24704.
- [27] C. M. Yamazaki, A. Yamaguchi, Y. Anami, W. Xiong, Y. Otani, J. Lee, N. T. Ueno, N. Zhang, Z. An, K. Tsuchikama, *Nat. Commun.* **2021**, *12*, 3528.
- [28] I. Dovgan, A. Ehkirch, V. Lehot, I. Kuhn, O. Koniev, S. Kolodych, A. Hentz, M. Ripoll, S. Ursuegui, M. Nothisen, S. Cianféran, A. Wagner, *Sci. Rep.* **2020**, *10*, 7691.
- [29] a) Y. Ogitali, T. Aida, K. Hagihara, J. Yamaguchi, C. Ishii, N. Harada, M. Soma, H. Okamoto, M. Oitate, S. Arakawa, T. Hirai, R. Atsumi, T. Nakada, I. Hayakawa, Y. Abe, T. Agatsuma, *Clin. Cancer Res.* **2016**, *22*, 5097–5108; b) G. D. Lewis Phillips, G. Li, D. L. Dugger, L. M. Crocker, K. L. Parsons, E. Mai, W. A. Blättler, J. M. Lambert, R. V. J. Chari, R. J. Lutz, W. L. T. Wong, F. S. Jacobson, H. Koeppen, R. H. Schwall, S. R. Kenkare-Mitra, S. D. Spencer, M. X. Sliwkowski, *Cancer Res.* **2008**, *68*, 9280–9290.
- [30] D. Panda, K. DeLuca, D. Williams, M. A. Jordan, L. Wilson, *PNAS* **1998**, *95*, 9313–9318.
- [31] A. B. Waight, K. Bargsten, S. Doronina, M. O. Steinmetz, D. Sussman, A. E. Prota, *PLoS one* **2016**, *11*, e0160890.
- [32] P. Liu-Kreyche, H. Shen, A. M. Marino, R. A. Iyer, W. G. Humphreys, Y. Lai, *Front. Pharmacol.* **2019**, *10*, 749.
- [33] a) C. D. Smith, X. Zhang, S. L. Mooberry, G. M. Patterson, R. E. Moore, *Cancer Res.* **1994**, *54*, 3779–3784; b) B. D.-M. Chen, A. Nakeff, F. Valeriote, *Int. J. Cancer* **1998**, *77*, 869–873.
- [34] Memorial Sloan Kettering Cancer Center, “SK-BR-3: Human Breast Cancer Cell Line (ATCC HTB-30)”, to be found under <https://www.mskcc.org/research-advantage/support/technology/tangible-material/human-breast-cell-line-sk-br-3>, **2024**.

Manuscript received: September 9, 2024

Revised manuscript received: October 24, 2024

Accepted manuscript online: October 27, 2024

Version of record online: November 13, 2024